# EFFECT OF AUSTENITE GRAIN MORPHOLOGY ON VARIANT SELECTION OF MARTENSITE TRANSFORMED FROM ULTRAFINE-GRAINED AUSTENITE

**H. R. Jafarian[1,*] and E. Borhani[2]**

\* *jafarian@iust.ac.ir*

[1] School of Metallurgy and Materials Engineering, Iran University of Science and Technology (IUST), Tehran, Iran.

[2] Department of Nanotechnology, Nano-Materials Science and Engineering group, Semnan University, Semnan, Iran.

**Abstract:** *In this research, variant selection of martensite transformed from ultrafine-grained (UFG) austenite fabricated by accumulative roll bonding (ARB) process and subsequent annealing was investigated with respect tomorphology of parentaustenitic phase. The results show that the original shape of austenite grain is very effective factor in determiningthe preferred variants of martensite transformed from the elongated ultrafine-grained austenite fabricated by 6-cycles via the ARB process. Annealing treatment of the austenitic samples subjected to the 6-cycle ARB processed at 873 K for 1.8 ks suppressed the variant selection by changing the morphology of austenite grains from elongated ultrafine-grains to fully-recrystallized and equiaxed fine-grains.*

## 1. INTRODUCTION

In recent years, bulky ultrafine grained (UFG) materials fabricated by severe plastic deformation with a mean grain size of less than 1 μm have been comprehensively studied, due to their superior mechanical properties [1-5]. A significant large area of grain boundaries per unit volume in UFG materials can affect martensitic transformation behavior as habit plates within martensitic structures cannot grow beyond grain boundaries. Previous studies clearly indicated that martensitic transformation can be significantly influenced by austenite grain size [6-11]. Umemoto and Owen [6] demonstrated that martensite transformation starting temperature ($M_s$) decreases with decrease of the austenite grain size. Maki et al. [7] studied the variety of martensite morphologies produced after being transformed from various grain sizes of austenite at different temperatures. Their results indicated that the refinement of austenite grains decreases the $M_s$, resulting to a change inmartensite morphology. Although several studies have been reported on the austenite grain-size effects [8-11], but there is no deep systematic study of the martensitic transformation from ultrafine-grained austenite.

It is well known that martensite usually satisfies Kurdjumov-Sachs (K-S) orientation relationship with respect to austenite ($\{111\}_A$ // $\{011\}_M$, $<101>_A$ // $<111>_M$, where subscripts A and M represent austenite and martensite, respectively) [12]. When the K-S relationship is maintained, 24 equivalent crystallographic variants of martensite can form from a single crystal of austenite. Table 1 summarizes the orientation relationships between the 24 crystallographic variants ($V_1$–$V_{24}$) of martensite and austenite under K-S orientation relationship.

When plastic deformation is introduced to austenite before martensitic transformation, the 24 variants of martensite do not form equally and some specific variants are preferentially formed, resulting to formation of transformation texture. This is so-called variant selection. Recently Chiba et al. [13] reported that variants of lenticular martensite habit planes that were closely parallel to compression planes which were favorably formed during ausforming of

**Table 1.** The 24 crystallographic variants of martensitefor the K-S orientation relationship

| Variant | Plane parallel | Direction parallel |
|---|---|---|
| $V_1$ | $(111)_A // (011)_M$ | $[\bar{1}01]_A // [\bar{1}\bar{1}1]_M$ |
| $V_2$ | | $[\bar{1}01]_A // [\bar{1}1\bar{1}]_M$ |
| $V_3$ | | $[01\bar{1}]_A // [\bar{1}\bar{1}1]_M$ |
| $V_4$ | | $[01\bar{1}]_A // [\bar{1}1\bar{1}]_M$ |
| $V_5$ | | $[1\bar{1}0]_A // [\bar{1}\bar{1}1]_M$ |
| $V_6$ | | $[1\bar{1}0]_A // [\bar{1}1\bar{1}]_M$ |
| $V_7$ | $(\bar{1}11)_A // (011)_M$ | $[0\bar{1}1]_A // [\bar{1}\bar{1}1]_M$ |
| $V_8$ | | $[0\bar{1}1]_A // [\bar{1}1\bar{1}]_M$ |
| $V_9$ | | $[\bar{1}0\bar{1}]_A // [\bar{1}\bar{1}1]_M$ |
| $V_{10}$ | | $[\bar{1}0\bar{1}]_A // [\bar{1}1\bar{1}]_M$ |
| $V_{11}$ | | $[110]_A // [\bar{1}\bar{1}1]_M$ |
| $V_{12}$ | | $[110]_A // [\bar{1}1\bar{1}]_M$ |
| $V_{13}$ | $(1\bar{1}1)_A // (011)_M$ | $[10\bar{1}]_A // [\bar{1}\bar{1}1]_M$ |
| $V_{14}$ | | $[10\bar{1}]_A // [\bar{1}1\bar{1}]_M$ |
| $V_{15}$ | | $[\bar{1}\bar{1}0]_A // [\bar{1}\bar{1}1]_M$ |
| $V_{16}$ | | $[\bar{1}\bar{1}0]_A // [\bar{1}1\bar{1}]_M$ |
| $V_{17}$ | | $[011]_A // [\bar{1}\bar{1}1]_M$ |
| $V_{18}$ | | $[011]_A // [\bar{1}1\bar{1}]_M$ |
| $V_{19}$ | $(11\bar{1})_A // (011)_M$ | $[\bar{1}10]_A // [\bar{1}\bar{1}1]_M$ |
| $V_{20}$ | | $[\bar{1}10]_A // [\bar{1}1\bar{1}]_M$ |
| $V_{21}$ | | $[0\bar{1}\bar{1}]_A // [\bar{1}\bar{1}1]_M$ |
| $V_{22}$ | | $[0\bar{1}\bar{1}]_A // [\bar{1}1\bar{1}]_M$ |
| $V_{23}$ | | $[101]_A // [\bar{1}\bar{1}1]_M$ |
| $V_{24}$ | | $[101]_A // [\bar{1}1\bar{1}]_M$ |

austenite. Lef et al. [14] investigated variant selection of mechanically induced martensite transformed from metastable austenite. They found that interaction energy between externally applied stress and lattice deformation can determine preferential marteniste variants based on Patel and Cohen's theory [15]. Recently, the present authors demonstrated that variant selection rule can be changed in severely deformed UFG austenite depending on amount of induced strain [16]. However, variant selection of martensite in UFG austenite has been rarely studied. So the aim of this study is to clarify the variant selection rules of martensite transformed from ultrafine-grained austenite with respect to morphology of austenite grains, i.e., austenite grain size and shape.

## 2. MATERIALS AND METHODS

An Fe-24Ni-0.3C (wt.%) alloy, of which chemical composition is shown in Table 2, was used in the present study. A cast ingot of the alloy was hot-rolled and then cold-rolled to make sheets with thickness of 1 mm. The sheets were austenitized at 1173 K for 3.6 ks for obtaining a fully recrystallized and coarse-grained austenite with a mean grain size of 35μm. To obtain ultrafine-grained austenite structures, the austenitized sheets were subjected to

**Table 2.** Chemical composition of the alloy studied (wt.%)

| Fe | C | Ni | Si | Mn | P | S | O | N |
|---|---|---|---|---|---|---|---|---|
| bal. | 0.29 | 24.09 | 0.01 | 0.07 | <0.005 | <0.0005 | 0.0008 | 0.0006 |

accumulative roll bonding (ARB) process. Figure 1 is a schematic illustration showing the principle of the ARB process [3]. In the ARB process, two pieces of the sheets 1 mm thick are stacked after degreasing and wire brushing the contact surfaces. The stacked sheets are roll-bonded by 50% reduction in one pass. Then, the roll-bonded sheet is cut into two, stacked to have the initial dimensions before rolling, and the procedures described above are repeated again. The ARB process can apply significant amount of plastic strain into materials, because the procedures can be repeated limitlessly. In order to prevent deformation-induced martensitic transformation during the present ARB process for obtaining fully austenitic structures, stacked sheets were held at 873 K, at which austenite phase of the studied alloy is stable, for 0.6 ks and subsequently roll-bonded. The roll-bonded sheets were immediately cooled in water. The roll-bonding was carried out under lubrication condition by the use of a two-high mill having a roll diameter of 310 mm.The ARB was repeated up to 6-cycle, so that total equivalent strain accumulated was 4.8. The 6-

cycle ARB processed specimens were annealed at 773, 823 and 873 K for 1.8 ks to obtain UFG austenite with partly recrystallized or fully recrystallized microstructures. The specimens subjected to the above mentioned treatments were cooled down to 77 K (in liq. $N_2$) to obtain thermally induced martensite.

The microstructures of the specimens before and after martensitic transformation were characterized by electron backscatter diffraction (EBSD) in a scanning electron microscope (SEM) equipped with a field-emission electron gun (Philips XL30S-FEG) operated at 15 kV. EBSD measurements were carried out with step size of 0.05μm which were smaller than the interval of austenite grain boundaries. The sections of the specimen for EBSD observation were polished mechanically and then electrolytically in a 900mL $CH_3COOH$+100mL $HClO_4$ solution at approximately 284K with a voltage of 20V. The obtained EBSD data were analyzed by TSL-OIM Analysis software Ver. 6.1.3.

## 3. RESULTS AND DISCUSSION

### 3. 1. Microstructure of Austenite

In Fig. 2, microstructure of austenite processed by ARB is illustrated by grain boundary and phase maps obtained by EBSD measurements and analysis. In the grain boundary maps, high angle boundaries with misorientation larger than 15° are drawn in black lines and low angle boundaries with misorientation between 2° and 15° are drawn in red lines. In addition, martensite and austenite phases are shown in pink and green colors, respectively. The grain boundary map of Fig. 2(a) indicates that the starting material consists of fully recrystallized and coarse grained austenite. The phase maps of Fig. 2(a)-(e) demonstrate 100% austenite structures, indicating that deformation-induced martensitic transformations did not occur during
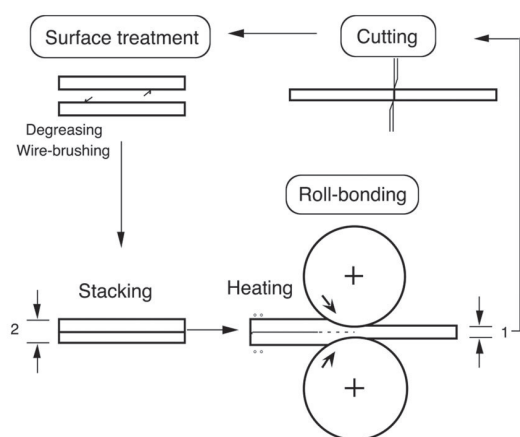


**Fig. 1.** Schematic illustration showing the principle of the accumulative roll bonding (ARB) [22].
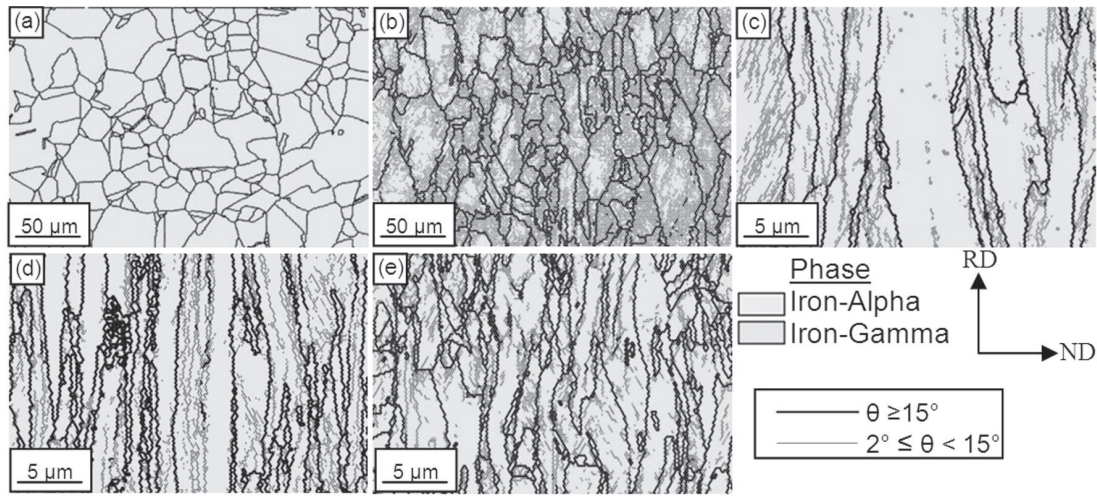
**21**

**Fig. 2.** (a)-(e) Grain boundary and phase maps of the starting material, 1-cycle, 2-cycle, 4-cycle and 6-cycle ARB processed specimens, respectively.

the ARB process at 873 K. The 1-cycle ARB process, corresponding to 50% rolling or an equivalent strain of 0.8, introduced a large amount of low angle boundaries into the austenite. Till 2-cycle of ARB process (75% rolling), the microstructures exhibit typical deformation microstructures which mainly involve pancake shape austenite grains having low angle boundaries (dislocation structures) inside. Increasing the number of ARB process up to 6-cycle causes significant grain refinement as shown in Fig. 2(e).



**Fig. 3.** (a)-(c) Grain boundary and phase maps of the specimens ARB processed by 6-cycle and annealed at 773, 823 and 873 K respectively.

The grain boundary and phase maps of austenite ARB processed by 6-cycle and subsequently annealed at 773, 823 or 873 K for 1.8 ks are shown in Fig. 3. The grain boundary map of the specimen annealed at 773K (Fig. 3(a)) shows that the microstructure still consists of UFG lamellar structure, indicating that annealing at 773 K does not cause recrystallization of austenite. Grain boundary map of Fig. 3(b) indicates that recrystallization occurs partly by increasing the annealing temperature to 823 K. The recrystallized regions are free of low angle boundaries. Annealing treatment at 873 K results in fully recrystallized and equiaxed austenite with mean grain size of 2.5 μm, as shown in Fig. 3(c). Moreover, phase maps superimposed on grain boundary maps show that no phase transformation occurs during annealing treatments.

Change in austenite grain size with increasing the number of ARB cycle and subsequent annealing is summarized in Fig. 4. Interception method was used to measure the grain size (or interval of boundaries) along normal direction (ND). Here, high angle boundaries were taken into account for the grain size ($d^{HAGB}$) measurement. The figure indicates that the grain size monotonously decrease with increasing strain (ARB cycle), and UFG austenite with mean grain size of 750 nm was obtained by 6-
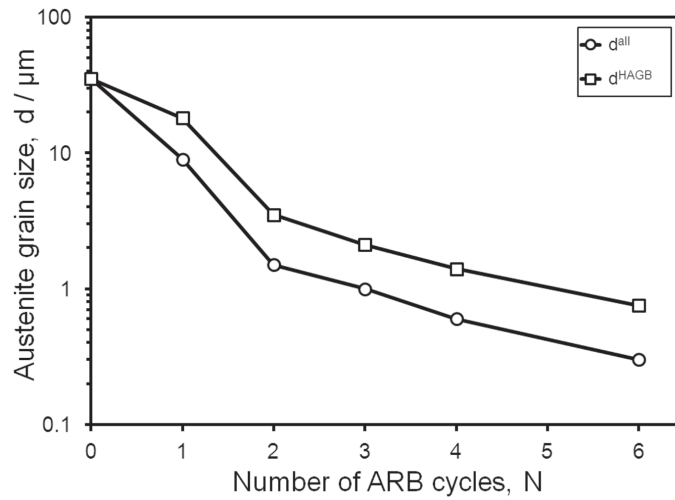
**22**

**Fig. 4.** Change in austenite grain size (boundary interval along ND) with the number of the ARB cycles and subsequent annealing.

cycle ARB process. Annealing treatment of austenite ARB processed by 6-cycle result in increasing of austenite grain size up to 2.5 µm at annealing temperature of 873 K as shown in Fig. 4.

### 3. 2. Variant Selection of Martensite

Figure 5(a) and (b) show an EBSD orientation map and corresponding $\{100\}_A$ pole figure of the starting material. The colors in the orientation map indicates the crystallographic directions of each point parallel to TD of the sheet (the normal direction of the observed plane), according to the stereographic triangle shown in the figure. The ideal $<100>_A$ axes of typical texture components in f.c.c crystal, i.e., Brass component ($\{110\}<112>_A$), Copper component ($\{112\}<111>_A$), S component ($\{123\}<634>_A$),
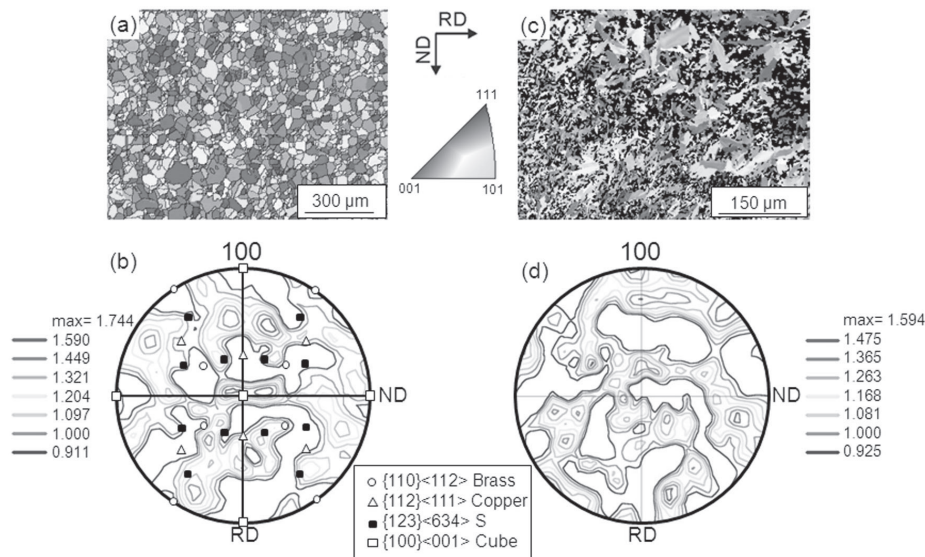


**Fig. 5.** ((a), (b)) EBSD orientation color map and $\{100\}$ pole figure of austenite before martensitic transformation in the starting material. ((c), (d)) EBSD orientation color map and $\{100\}$ pole figure of martensite after martensitic transformation in the starting material.

process and shape deformation [16].

As explained, the austenite after 6-cycle of ARB exhibits lamellar structure elongated along the rolling direction (RD) of the sheet. The average interval of high angle boundaries along the ND of the sheet is about 750 nm. This is a typical ultrafine grained structure fabricated by the ARB process. Since martensite plate cannot grow across high angle boundaries of austenite, it seems that the lamellar shape (elongated along RD) of the ultrafine-grained austenite (Fig. 2(c)) affects the variant selection of martensite transformed from the 6-cycle ARB processed specimen. On this basis, habit plane orientations for the 24 variants of martensiteare plotted on the pole figure of which coordinate system corresponds to Brass orientation (RD // $[2\,\overline{1}1]_A$, ND // $[011]_A$), as shown in Fig. 7. The pole figure of Fig. 7 reveals that the normal directions of habit planes for the preferentially formed variants of martensite transformed from the 6-cycle ARB processed specimen having elongated ultrafine-grained austenite (represented by red color) are nearly parallel to ND ($V_6$, $V_{16}$) or TD ($V_{19}$, $V_{21}$, $V_{22}$, $V_{24}$). The martensite plates of which normal directions of habit planes are parallel to ND or TD can grow along the elongated direction of the
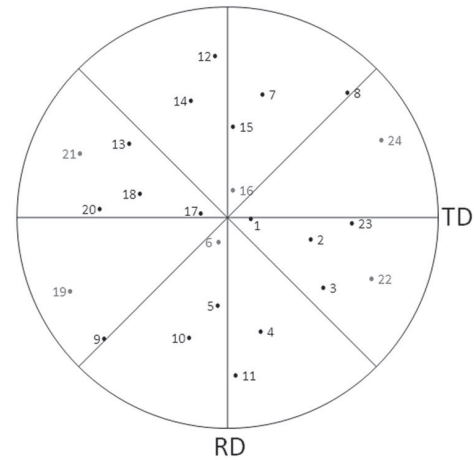


**Fig. 7.** A pole figure showing the habit plane orientation for the 24 variants of martensite. The preferentially formed variants of martensite transformed from the 6-cycle ARB processed specimen having elongated ultrafine-grained austenite are indicated by red color. The coordinate system of the pole figure corresponds to the Brass texture (RD = $[2\,\overline{1}\,1]_A$, ND = $[011]_A$), which was found in the 6-cycle ARB processed austenite. The numbers indicate the positions of the habit plane orientation for the 24 variants of martensite transformed from the austenite with exact Brass orientation ($(011)\,[2\,\overline{1}\,1]_A$).

ultrafine-grained austenite in the 6-cycle ARB processed specimen. Therefore, it can be



**Fig. 8.** EBSD orientation color maps and $\{100\}_A$ pole figures of austenite in ((a), (b)) the specimen 6-cycle ARB processed and then annealed at 773 K for 1.8 ks, and ((c), (d)) the specimen 6-cycle ARB processed and then annealed at 873 K for 1.8 ks.

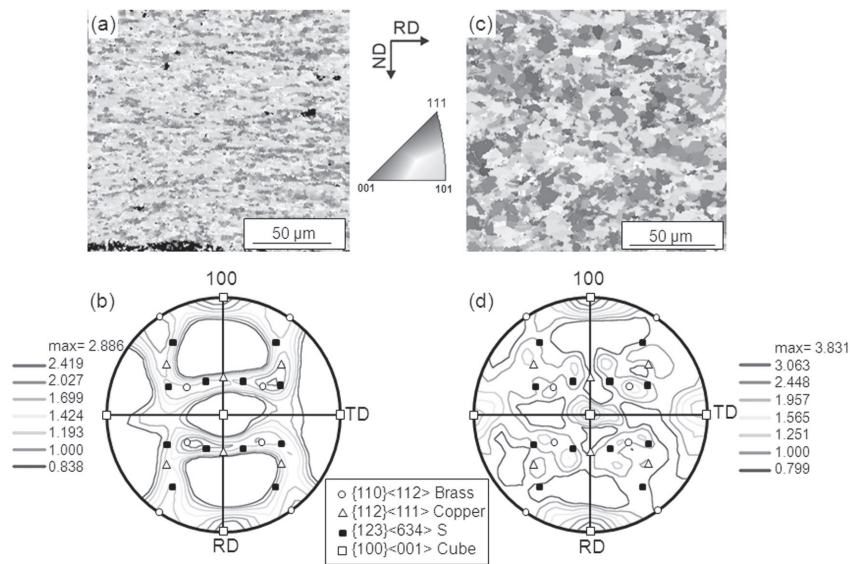concluded that in the case of the 6-cycle ARB processed specimen having elongated ultrafine-grained austenite, austenite grain shape significantly affects the variant selection in martensitic transformation.

Figure 8(a) and (b) shows an EBSD orientation map and corresponding $\{100\}_A$ pole figure of the 6-cycle ARB processed specimen after annealing at 773 K for 1.8 ks. The 6-cycle ARB processed specimen still consists of elongated ultrafine-grained austenite after annealing at 773 K. In addition, Brass texture is kept after annealing at 773 K. This is because annealing at 773 K causes no recrystallization but only recovery, as explained. In contrast, recrystallization occurs by annealing at 873 K for 1.8 ks, resulting in the development of Cube texture as shown in Fig. 8(c) and (d).

Figure 9 (a) and (b) displays the EBSD orientation map and corresponding $\{100\}_M$ pole figure of martensite transformed from the austenite 6-cycle ARB processed and then annealed at 773 K for 1.8 ks having elongated ultrafine-grains. The positions of the ideal $<100>_M$ axes for the 24 variants of martensite

transformed from the austenite with exact Brass orientation ($(011) [2\ \bar{1}\ 1]_A$) are plotted in Fig. 9(b). The preferentially formed variants of martensite transformed from the 6-cycle ARB processed specimen after annealing at 773 K are $V_6$, $V_{16}$, $V_{19}$, $V_{21}$, $V_{22}$ and $V_{24}$, which are completely the same as those transformed from the 6-cycle ARB processed specimen (Fig. 6(d)). This fact supports the previous conclusion that the variant selection rule is determined by austenite grain shape, and not by interaction energy between the residual stress of austenite and shape deformation, when the austenite has elongated ultrafine-grained structures because the residual stress of austenite, which is inherited during the 6-cycle ARB process, is released to some extent by annealing at 773 K.

Figure 9(c) and (d) show an EBSD orientation map and corresponding $\{100\}_M$ pole figure of martensite transformed from the austenite 6-cycle ARB processed and then annealed at 873 K for 1.8 ks having equiaxed (recrystallized) fine-grains. Although the austenite 6-cycle ARB processed and then annealed at 873 K for 1.8 ks has the strong cube texture (Fig. 8(c)), the
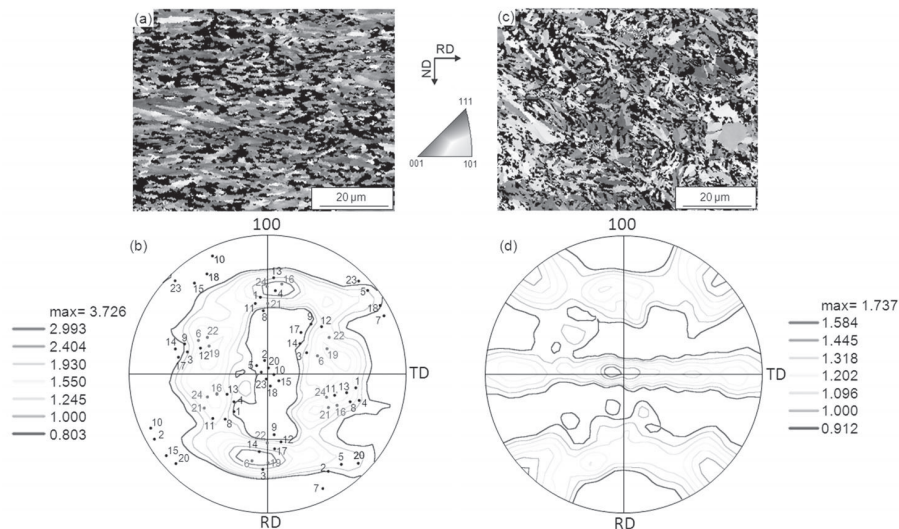


**Fig. 9.** EBSD orientation color maps and {100}M pole figures of martensite transformed from ((a), (b))the specimen 6-cycle ARB processed and thenannealed at 773 K for 1.8 ks, and ((c), (d)) the specimen 6-cycle ARB processed and thenannealed at 873 K for 1.8 ks.The positions of the ideal $<100>_M$ axes for the 24 variants of martensite transformed from the austenite with exact Brass orientation ($(011) [2\ \bar{1}1]_A$) are shown in by the numbers (b). The preferential variants are indicated by red color.

intensities of martensite in the pole figure of Fig. 9(d) are very weak. This indicates that there is no variant selection of martensite transformed from the austenite having fully recrystallized and eqiaxed grains even when austenite grain size is very fine.

## 4. CONCLUSIONS

In this paper, effect of austenite grain morphology on variant selection of martensite transformed from the ARB processed specimens having elongated ultrafine-grained austenite (the 6-cycle ARB processed specimen) and equiaxed fine-grained austenite (the specimen 6-cycle ARB processed and annealed at 873 K for 1.8 ks), was studied in the Fe-24Ni-0.3C alloy. The conclusions are summarized as follows:

1. The ARB process resulted in ultra-grain refinement of austenite. The obtained ultrafine grained (UFG) austenite consisted of the lamellar grains elongated along the rolling direction (RD) with mean grain thickness of 750 nm after 6-cycle of the ARB process. The starting material had random texture, while the 6-cycle ARB processed austenite exhibited the development of strong Brass component.

2. The variant selection in martensitic transformation from the 6-cycle ARB processed specimen having elongated ultrafine-grained austenite indicated that the elongated grain shape played an important role for the variant selection of martensite, i.e., the martensite plates which can grow along the elongated direction of the ultrafine-grained austenite were preferentially formed.

3. Annealing treatment of the 6-cycle ARB processed specimen at 773 K for 1.8 ks induced no recrystallization but only recovery of austenite, resulting in the same transformation texture and variant selection rule with those in the 6-cycle ARB processed specimen. In contrast, annealing treatment of the 6-cycle ARB processed austenite at 873 K for 1.8 ks suppressed the variant selection by changing the austenite structure from elongated ultrafine-grains to fully-recrystallized and equiaxed fine-grains.

## REFERENCES

1. Valiev, R. Z., Krasilnikov, N. A., Tsenev, N. K., "Plastic deformation of alloys with submicro-grained structure", Mater. Sci. Eng.A, 1991,137, 35.

2. Horita, Z., Smith, D. J., Furukawa, M., Nemoto, M., Valiev, R. Z., Langdon, T. G., "An investigation of grain boundaries in submicrometer-grained Al-Mg solid solution alloys using high-resolution electron microscopy", J. Mater. Res., 1996,11, 1880.

3. Saito, Y., Tsuji, N., Utsunomiya, H., Sakai, T., "Novel ultra-high straining process for bulk materials development of the accumulative roll-bonding (ARB) process", ActaMater., 1999, 47, 579.

4. Valiev, R. Z., Zehetbauer, M. J., Estrin, Y., Höppel, H. W., Ivanisenko, Y., Hahn, H., Wilde, G., Roven, H. J., Sauvage, X., Langdon, T. G., "The Innovation Potential of Bulk Nanostructured Materials", Adv. Eng. Mater., 2007, 9, 527.

5. Tsuji, N., "Unique Mechanical Properties of Nano-Structured Metals", J. of Nanosci. andNanotech.,2007, 7,3765.

6. Umemoto, M., Owen, W. S., "Effects of austenitizing temperature and austenite grain size on the formation of athermalmartensite in an iron-nickel and an iron-nickel-carbon alloy", Metall. Trans.,1974, 5, 2041.

7. Maki, T., Shimooka, S., Fujiwara, S., Tamura, I., "Formation temperature and growth behavior of thin plate martensite in Fe-Ni-C alloys", Trans. JIM 1975, 16, 35.

8. Tadaki, T., Murai, Y., Koreeda, A., Nakata Y., Hirotsu, Y., "Structure and phase transformation of nano-scale particles of Fe-Ni alloys", Mater. Sci. and Eng.A,1996, 217–218, 235.

9. Takaki, S., Fukunaga, K., Syarif, J., Tsuchiyama, T., "Effect of grain refinement on thermal stability of metastable austenitic steel", Mater. Trans. 2004, 45, 2245.

10. Kitahara, H., Tsuji, N., Minamino, Y., "Martensite transformation from ultrafine grained austenite in Fe–28.5 at.% Ni", Mater.

Sci. and Eng.A 2006, 438–440, 233.

11. Jafarian, H. R., Borhani, E., Shibata, A., Terada, D., Tsuji, N., "Martensitic Transformation from Ultrafine Grained Austenite Fabricated by ARB in Fe-24Ni-0.3 C", Mater. Sci. Forum,2011, 667-669, 361.

12. Kurdjumov, G., Sachs, G. Z., Phys, 1930, 64, 325.

13. Chiba, T., Miyamoto, G., Furuhara, T., "Variant selection of lenticular martensite by ausforming", Scripta Mat.2012, 67, 324.

14. Lee, S. H., Kang, J. Y., Han, H. N., Oh, K. H., Lee, H. C., Suh, D. W., Kim, S. J., "Variant selection in mechanically-induced martensitic transformation of metastable austenitic steel", ISIJ International, 2005, 45,1217.

15. Patel, J. R., Cohen, M., "Criterion for the action of applied stress in the martensitic transformation", Acta Metal. 1953, 1, 531.

16. Jafarian, H. R., Borhani, E.,Shibata A., Tsuji, N., "Variant selection of martensite transformation from ultrafine-grained austenite in Fe-Ni-C alloy Journal of Alloys and Compounds", accepted, 2012.[Doi: 10.1016/ j.jallcom. 2012.04.057]

17. Kundu, S., "Prediction of transformation texture under complex rolling condition", Mater.Sci. Eng.A,2009, 516, 290.